Reactive transport modeling in heterogeneous porous media with dynamic mesh optimization

As Published: https://doi.org/10.1007/s10596-020-10009-y

Publisher: Springer International Publishing

Persistent URL: https://hdl.handle.net/1721.1/131986

Version: Author's final manuscript: final author's manuscript post peer review, without publisher's formatting or copy editing

Reactive transport modeling in heterogeneous porous media with dynamic mesh optimisation

Cite this article as: , Reactive transport modeling in heterogeneous porous media with dynamic mesh optimisation, *Computational Geosciences* doi: 10.1007/s10596-020-10009-y

0
if
tex.enableprimitives
thenΩtex.enableprimitives(Ω'pdf@',Ω'primitive',
'if-
prim-
i-
tive',
'pdf-
draft-
mode','draftmode'Ω)Ωtex.enableprimitives('',
'lu-
aescapestring')ΩendΩ

Reactive transport modeling in heterogeneous porous media with dynamic mesh optimisation

A. Yekta [1] · P. Salinas[2,*] · S. Hajirezaie[3] · M. A. Amooie[4] · C. C. Pain[2] · M. D. Jackson[2] · C. Jacquemyn[2] · M. R. Soltanian[1,5]

Received: date / Accepted: date

Abstract This paper presents a numerical simulator for solving compositional multiphase flow and reactive transport. The simulator was developed by effectively linking IC-FERST (Imperial College Finite Element Reservoir SimulaTor) with PHREEQCRM. IC-FERST is a next-generation three-dimensional reservoir simulator based on the Double-Control-Volume Finite Element method and dynamic unstructured mesh optimization and is developed by the Imperial College London. PHREEQCRM is a state-of-the-art geochemical reaction package and is developed by the United States Geological Survey. We present a step-by-step framework on how the coupling is performed. The coupled code is called IC-FERST-REACT and is capable of simulating complex hydrogeological, biological, chemical, and mechanical processes occurring including processes occur during CO_2 geological sequestration, CO_2 enhanced oil recovery and geothermal systems among others. In this paper, we present our preliminary work as well as examples related to CO_2 geological sequestration. We performed the model coupling through developing an efficient application programming interface (API). IC-FERST-REACT inherits high-order methods and unstructured meshes with dynamic mesh optimization from IC-FERST. This reduces the computational cost by placing the mesh resolution where and when necessary and it can better capture flow instabilities if they occur. This can have a strong impact on reactive transport simulations which usually suffer from computational cost. From PHREEQCRM the code inherits the ability to efficiently model geochemical reactions. Benchmark examples are used to show

[1]Department of Geology, University of Cincinnati, Cincinnati, OH, USA
[2]Novel Reservoir Modelling and Simulation Group, Department of Earth Science and Engineering, Imperial College London, UK
[3]Department of Civil Engineering, Princeton University, NJ, USA
[4]Department of Chemical Engineering, Massachusetts Institute of Technology, Cambridge, Massachusetts, USA
[5]Department of Environmental Engineering, University of Cincinnati, Cincinnati, OH, USA
[*]Corresponding author: Pablo Salinas, pablo.salinas@imperial.ac.uk

the capability of IC-FERST-REACT in solving multiphase flow and reactive transport.

Keywords Modeling · Multiphase flow · Reactive transport · IC-FERST · PHREEQCRM · Dynamic mesh optimization

1 Introduction

Chemical and biological reactions play a significant role in various subsurface flow and mass transport problems. Reactions can affect fluid phase properties and can also change subsurface petrophysical (e.g., permeability, porosity) and geochemical attributes (e.g., surface area of minerals). The importance as well as the difficulty to properly model chemical and biological reactions means that a great deal of effort has been put over the years to understand how reaction affects fluid flow in porous media and how to model it properly [23, 25, 26, 28, 40, 44, 45, 47–50]. For example, geochemical reactions are important in various petroleum engineering related processes such as alkaline species injection into oil reservoirs in order to generate in-situ surfactants due to reactions with the oil [21]. These reactions eventually reduce the interfacial tension between the oil and water resulting in a higher oil recovery [24]. Another example is geological sequestration of carbon dioxide (CO_2) in brine-saturated aquifers. The injected CO_2 dissolves in brine and produces bicarbonic acid (pH is 3). This low pH results in mineral dissolution and precipitation over short and long time-scales [42]. Reactions are coupled and can directly affect the transport processes, including advection, dispersion and diffusion. However, understanding and predicting such complex and coupled processes in subsurface systems and their quantitative interpretation (for both laboratory- and field-scale experiments) need coupled (multi-phase) flow, mass transport, and geochemical reaction tools. There are several applications in which (bio)geochemical reactions play major role. This include for example bioremediation, biodegradation, natural attenuation, nutrient cycling within aquatic interfaces (e.g., groundwater and surface water interaction zone) [35, 43, 57].

Deep brine-saturated aquifers offer a large storage capacity for CO_2 sequestration [15]. Although CO_2 storage during geologic sequestration is generally believed to be secure under different conditions, there is still a need to accurately quantify the possibility of CO_2 leakage back to shallower depth which can impact potable aquifers [7]. Accurate numerical simulations of CO_2-brine multiphase flow and reactive transport within heterogeneous faulted domains will help assessing the possible impacts of rock heterogeneity, fractures and faults on CO_2 migration and reactivity in subsurface systems. However, heterogeneity is present across different scales and fractures or faults are narrow (high aspect-ratio) compared other parts of an aquifer. Therefore, simultaneously modelling all these length-scales is challenging. Specifically, representing fractures using structured grids is quite difficult. Unstructured grids can ease

this process by allowing use of different elements sizes for the different length-scales [16]. Adapting element size throughout simulations can significantly add to this advantage. In this paper, we focus on the numerical experiments related to CO_2 geological sequestration.

There are now powerful multiphase flow and reactive transport codes available including PFLOTRAN, TOUGHREACT, HYDROGEOCHEM, CrunchFlow, CMG-GEM, STOMP/eSTOMP, CSMP++GEM, HYTEC and NUFT [13,14,46,53–56,58,59]. Steefel et al. [44] presented a comprehensive review of different modern numerical reactive transport codes, in addition to a detailed background information about the mathematical and numerical formulations. These models are great tools. However, they mainly use classical approaches for simulating multiphase flow and reactive transport problems, which is using finite differences (FD) on structured grids and finite volumes (FV) on unstructured grids. An alternative to FD and FV methods is the use of finite elements (FE) combined with control volumes (CV), known as the control volume finite element method (CVFEM) [8,10,11,16]. This approach has the flexibility of FE discretization, suitable for representing complex geologic features, as well as capabilities of control-volume (CV) methods in generating stable, locally mass-conservative solutions. Examples of multiphase porous media and reactive transport codes are FEHM, developed by Los Alamos Laboratory [61] and OpenGeoSys developed by the Helmholtz center for enviromental research [20]. Here, to model the multiphase flow the code Imperial College Finite Element Reservoir Simulator (IC-FERST) is used. IC-FERST uses a more robust version of the the classical CVFEM named Double Control Volume Finite Element Method (DCVFEM) [39] as well as Dynamic Mesh Optimisation [29]. Zhang et al. [60] also looked at reducing the computational effort required by reactive codes by reducing the required degrees of freedom by using an advanced Adaptive Mesh Refinement (AMR) approach.

IC-FERST is publicly available under the terms of the Affero General-Purpose License (AGPL). IC-FERST has been fully parallelized with MPI [38]. It has been tested on the U.K. national supercomputer Archer. Importantly, IC-FERST can solve for Darcy as well as Navier-Stokes formulations in two- and three-dimensions. Another powerful feature in IC-FERST is that it can be coupled to Solidity (a finite element – discrete element to solid mechanics code) to model mechanics of the fluid and rock interactions [27]. A non-isothermal version of IC-FERST to model geothermal reservoirs is under development. Motivated by IC-FERST advanced features and aforementioned ongoing efforts, we believe it is essential to add reactive transport capabilities to IC-FERST in order to fully exploit its advantages for complex subsurface problems. This is the goal of this work in which we perform coupling between IC-FERST and a geochemical reaction package, PHREEQC.

PHREEQC [32] is a public domain geochemical reaction package developed by the US Geological Survey (USGS). It is capable of modeling wide range of biogeochemical reactions and one-dimensional (1D) advective and dispersive transport processes. PHREEQC is based on the equilibrium chemistry of aqueous solutions and considers interactions of the aqueous solutions with

minerals, gases, solid solutions, exchangers, and sorption surfaces. PHREEQC has the capability of calculating kinetic reactions with user-specifiable rate equations. Some of the powerful features of PHREEQC include speciation and saturation indices (SI) of minerals calculations, mixing of different solutions, and reaction path modelling. Different thermodynamic databases are available within PHREEQC. Detailed description of PHREEQC can be found in [31,32].

There are different versions of PHREEQC available that facilitate coupling flow and transport codes to biogeochemical reactions. For example, IPHREEQC has PHREEQC capabilities with wrappers for C and FORTRAN in order to ease the integration of PHREEQC into other codes [4]. PHREEQCRM is a C++ class that is based on IPHREEQC and it was written specifically for implementing reaction calculations within different flow and mass transport simulators. PHREEQCRM has all of the capabilities of PHREEQC reaction calculations [33]. Importantly, PHREEQCRM has built-in parallelization by either OpenMP or MPI. Here we chose PHREEQCRM as a reaction engine for IC-FERST. PHREEQCRM geochemical reaction module is based on an operator-splitting approach, designed specifically to perform equilibrium and kinetic reaction calculations for transport simulators.

Modeling mass transport processes coupled with geochemical reactions has been subject of rigorous research. This is in part due to the difficulties in coupling transport and reactions. The main problem is related to the size and nonlinearity of the resulting system of equations [22]. There are mainly two methodologies for solving transport and reaction processes together: the sequential and the simultaneous or fully-coupled approach. As clear from its name, in the sequential approach the flow and the chemical reactions are solved sequentially [6, 51]. Iterations could also be applied between transport and reaction until convergence is achieved. The coupled method essentially involves solving transport and reaction equations simultaneously with Newton-Raphson method [48,49]. **In this study, we used the sequential approach by coupling PHREEQCRM and IC-FERST in a non-iterative framework. The sequential non-iterative approach (SNIA) is a commonly used coupling scheme in reactive transport modeling. [3] compared five coupling schemes for a reactive transport benchmark. In their work, the SNIA proved good efficiency and reasonable error magnitude. One problem associated with SNIA is mass error induced by changes in petrophysical properties as a result of dissolution and precipitation. In the results presented here the reaction rate is small and it does not affect the characteristics of the rock. Nonetheless, for other circumstances a two-way coupling would be required to ensure that mass conservation issues are accounted for properly.**

Our goal is to develop a reaction engine within IC-FERST in the near future. In order to couple IC-FERST and PHREEQCRM, we have developed an application programming interface (API) in which IC-FERST is used as the compositional multiphase flow engine and PHREEQCRM is used as the reaction engine through a SNIA approach. In what follows, first, we present a brief overview of IC-FERST. Then we present the way the developed API

works. We will then present numerical test cases against PHREEQC as well as some examples related to mineral dissolution during CO_2 sequestration in fractured and faulted aquifers. Note that PHREEQC and PHREEQCRM are well-documented and the readers are referred to PHREEQ's user manual as well as website for more information [30].

2 Fluid model

For the space discretization IC-FERST uses a double-control-volume-finite-element method (DCVFEM). The DCVFEM is based on the classical control-volume-finite-element method (CVFEM) [10] in which the pressure and velocity are discretized using finite elements and fields that need to be conserved are discretized using control **volumes in the control-volume mesh** (created by connecting the barycenter of the elements with the midpoint of the edges of those elements). In the DCVFEM, the pressure is discretized using finite volumes instead of finite elements, enabling us to obtain stable solutions with challenging meshes. Here, the element pair used is the $P_0DGP_1(CV)$, i.e. the velocity has zeroth order discontinuous representation while pressure and component mass fractions have first order representation. Time is discretized using a θ-method where θ varies between 0.5 (Crank-Nicholson) and 1 (implicit order) based on the total variational diminishing) (TVD) criterion. Fluxes are calculated using a second-order Taylor expansion series at the boundary between CVs, in this way a high order flux is obtained. Here we present a summary of the equations implemented in IC-FERST as this has been described previously [12, 16, 39]. **Darcy law is written as:**

$$\mu_\alpha S_\alpha \left(\mathcal{K}_{r_\alpha}\mathbf{K}\right)^{-1}\mathbf{u}_\alpha = -\nabla p + \mathbf{s}_{u\alpha}, \tag{1}$$

where p is pressure, μ_α the viscosity, S_α the saturation of phase α, $\mathbf{u}_\alpha$ is the saturation weighted velocity defined as the Darcy velocity divided by the saturation, K the permeability, $\mathcal{K}_{r_\alpha}$ the relative permeability and $\mathbf{s}_{u\alpha}$ the source term that may contain gravity or capillary pressure effects, not considered here for simplicity. The saturation equation, can be written as:

$$\phi\frac{\partial S_\alpha}{\partial t} + \nabla\cdot(\mathbf{u}_\alpha S_\alpha) = s_{cty,\alpha}, \tag{2}$$

where ϕ is the porosity and $s_{cty,\alpha}$ is a source term. To close the system the summation constrain is added:

$$\sum_{\alpha=1}^{n} S_\alpha = 1, \quad \forall\, n, \tag{3}$$

where n is the number of phases. To solve for components, we include the transport equation for components:

$$\phi\frac{\partial C_c}{\partial t} + \nabla\cdot(\mathbf{u}_\alpha C_c) = q_c, \tag{4}$$

where q_c is a volumetric source term, C_c the concentration of component c. The components are also constrained by:

$$\sum_{\alpha=1}^{n} C_\alpha = 1, \quad \forall\, n_c, \tag{5}$$

where n_c is the total number of components.

In IC-FERST-REACT, IC-FERST works as a transport part of our coupling procedure (Figure 1), in this paper no source terms nor diffusion or dispersion are considered. Note that this is just to simplify the simulations as the interest here is to focus on the coupling and validation with PHREEQC only, see [1,16,18,27,37] for examples with multiphase flow, geothermal, saline intrusion, solid-fluid coupling and parallel performance study using MPI. Due to the flexibility introduced by the use of unstructured grids, fractures and other geological features are represented and modelled explicitly, i.e. no dual-porous formulation is used.

2.1 Surface-based modelling for geological representation

IC-FERST uses surface-based modelling to represent the different petrophysical properties and unstructured meshes to discretize the domain. In surface-based modelling, the petrophysical properties are defined using discrete values bounded by surfaces [17, 36]. In this approach, geological representation and the mesh used to discretize the domain are independent. Initially, the geology can be represented using, for example, NURBS (Non-Uniform Rational B-Spline) surfaces. Using NURBS enables to use off-the-shelf CAD programs to manipulate the surfaces, allowing us to efficiently create complex models [17]. Once the geological model is generated, a mesh is created so the geological model can be read by the numerical simulator, in this case IC-FERST. The procedure is better detailed in [17].

2.2 Dynamic mesh optimization for porous media flow

IC-FERST has the capability to adapt the mesh to focus the mesh resolution where and when necessary while coarsening the mesh elsewhere. This enables IC-FERST to reduce the number of elements required to solve for a given model. The dynamic mesh optimization (DMO) library used is the one detailed in [29]. The mesh is optimized considering an approximation of the error based on the Hessian of the fields of interest. In that way, an approximation of the error can be estimated, and a mesh can be optimized to minimize that error. **Thus, the user can select the desired precision of some fields, for example one percent**. To modify the given mesh, elements can be added, removed or modified internally by moving nodes or swapping edges.

Once an optimal mesh is obtained, the fields need to be interpolated from the old mesh to the new mesh. Many methods are available to perform this operation. Here, we use the Galerkin projection [9] since it ensures mass conservation. More importantly for porous media flow is the use of surface-based modeling to represent the geology [17]. Surfaces are not altered during the modification of the mesh; therefore the geology of the model is unaffected despite the fact that the mesh has changed. Moreover, this simplifies the mesh-to-mesh interpolation of geological properties such as porosity or permeability, which can be prohibitively expensive since a process of up-, down- or cross-scaling should be performed, instead a direct imposition of the values can be applied.

3 Coupling procedure

An API is developed for couple flow, transport, and chemical reactions by applying SNIA scheme (Figure 1). The fields associated with the fluid modelling is controlled by IC-FERST, this includes, pressure, velocity, saturation and concentration. The geochemistry part is solved with PHREEQCRM (see Figure 1). The basic task for the PHREEQCRM reaction engine is to take component concentrations for each CV from IC-FERST, and solve the geochemical reactions. Then PHREEQCRM returns updated component concentrations to IC-FERST. For each grid cell, PHREEQCRM updates the concentrations of all possible reactants (i.e., dissolved species, minerals, exchangers, surface complexes, gas phases, solid solutions, and user-defined kinetically controlled reactants). It is important to note that PHREEQCRM only requires local information regarding each CV, this implies that the use of DMO does not introduce any constrain to the procedure at this stage and also parallelisation of the procedure is straightforward since only IC-FERST requires communication between nodes.

IC-FERST-REACT controls the memory and the calls to both IC-FERST and PHREEQCRM and therefore these do not communicate between them directly. Here, we have only considered for PHREEQCRM to compute new concentration fields, nonetheless potentially more fields could be recalculated by PHREEQCRM and subsequentally provided to IC-FERST to perform the flow transport. The procedure of the coupling by IC-FERST-REACT is as follows:

1. IC-FERST-REACT runs to configure the simulation domain and the related flow and transport parameters initializing IC-FERST and PHREEQCRM. Boundary and initial conditions are applied for the transport and the reaction model.
2. After the initialization step, the process first enters the iteration loop of the split operator (yellow box in Figure 1).

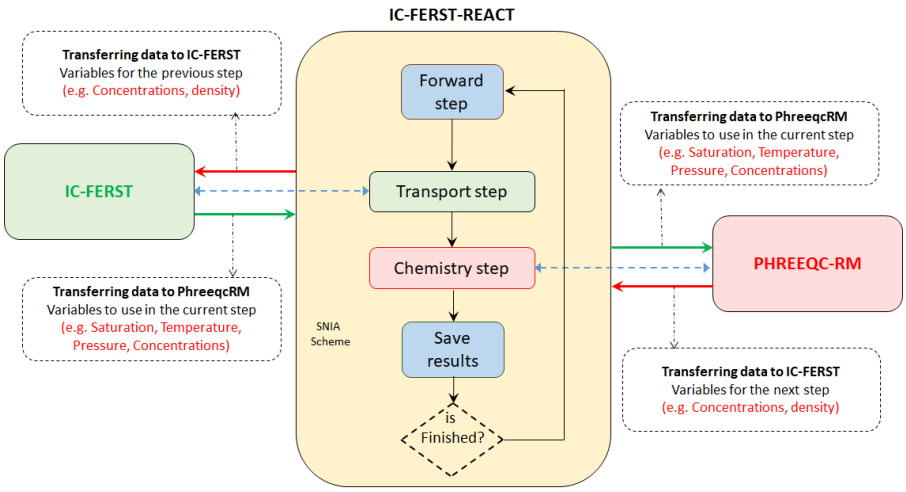

Fig. 1: IC-FERST-REACT flowchart showing IC-FERST and PHREEQCRM coupling. In each step, all variables are passed from IC-FERST to PHREEQCRM for cell-based geochemical calculations. Updated variables are transferred back to IC-FERST for the next transport step.

3. IC-FERST-REACT provides IC-FERST with the current pressure, velocity and concentration (green box within the yellow box in Figure 1).
4. IC-FERST updated pressure, velocity and concentration to the next time-level (green box outside the yellow box in Figure 1).
5. IC-FERST-REACT provides the fields already calculated by IC-FERST to PHREEQCRM to perform the reaction calculations (red box within the yellow box in Figure 1).
6. PHREEQCRM computes the new concentration fields for each grid cell that contains physical amounts (moles) of solution and chemical properties representing the reactive processes of interest. In this process, the transport is not considered (red box outside the yellow box in Figure 1).
7. IC-FERST-REACT advances one time-level and repeats the operation until the final time-level is reached.

In SNIA no iteration is performed between IC-FERST and PHREEQCRM. This results in a fast-one-way coupling procedure, which has the same limitations as other SNIA approaches in terms of physics applicable and CFL condition. A possibility to include a fully-coupled approach is to use SIA to ensure that we see the effect of geochemical reactions on flow field accurately. This is our ongoing work and is outside the scope of this paper.

4 Numerical experiments

Four experiments with increasing complexity are presented to show the validity and some capabilities of IC-FERST-REACT. In 4.1 we test the integrated code (IC-FERST-REACT) against one of PHREEQC's benchmark problem which is a 1D single-phase reactive-transport model. Note that both IC-FERST and PHREEQC have been tested in prior work. In 4.2 a validation experiment considers a homogeneous limestone composed only of calcite in which we inject to it an acidified fluid. For 4.3 we present a multiphase example in which CO_2 is injected in a fractured limestone initially filled with water. Finally, in 4.4 we consider CO_2 injection in a faulted aquifer. For this latter example, we show the DMO capability of IC-FERST-REACT. In all the cases the non-linear solver iterates until the difference between non-linear iterations of the concentration is below 1 percent and also in the case of model 4.3, the saturation is also checked with that precision. **Table 1 shows the fluid and geometrical parameters for the four test cases. In the numerical model with two phases Model 4.3, the relative permeability of each phase is given by the Brooks-Corey model [2]:**

$$k_{rw}\left(S_w\right) = K^e_{rw}\left(\frac{S_w - S_{wirr}}{1 - S_{wirr} - S_{nwr}}\right)^{n_w}, \tag{6}$$

$$k_{rnw}\left(S_w\right) = K^e_{rnw}\left(\frac{S_{nw} - S_{nwr}}{1 - S_{wirr} - S_{nwr}}\right)^{n_{nw}}, \tag{7}$$

where S_{nwr}, S_{wirr} and K^e_{rnw} , K^e_{rw} are the immobile fractions and the the end-points of the non-wetting and wetting phase respectively.

Property	4.1	4.2	4.3	4.4
$\mu_w = \mu_{nw}$ (Pa s)	10^{-3}	10^{-3}	10^{-3}	10^{-3}
K^e_{rw}	N/A	N/A	0.3	N/A
K^e_{rn}	N/A	N/A	0.8	N/A
$S_{nwr} = S_{wirr}$	N/A	N/A	0.2	N/A
$n_w = n_{nw}$	N/A	N/A	2.0	N/A
ϕ_{low}	N/A	N/A	0.2	0.1
ϕ_{high}	0.2	0.2	1.0	0.2
k_{low}	N/A	N/A	9.87×10^{-14}	9.87×10^{-16}
k_{high}	9.87×10^{-10}	9.87×10^{-10}	9.87×10^{-10}	9.87×10^{-13}
L (m)	0.08	1	0.52	220
H (m)	0.01	0.1	0.5	100
W (m)	N/A	0.1	0.05	82
$\#Elements$	150	150	30912	30000

Table 1: Model fluid set-up for the test cases 4.1 – 4.4.

4.1 Cation exchange example

Through this example IC-FERST-REACT is verified against the PHREEQC for a 1D single-phase flow and reactive (cation exchange) transport problem. The problem is from PHREEQC User's Guide and has been used in the literature to test several reactive transport models [19]. The problem is simulation of the transport of solutes in a saturated column, see 1 for domain a fluid properties. The column is flushed with a calcium-chloride ($CaCl_2$) solution. Processes of interest are advection of ionic species in the column containing a cation exchanger. The initial solution of the column contains 1.0 mmol Na^+, 0.2 mmol K^+, and 1.2 mmol NO_3^- per kilogram of water. The inlet solution has a composition of 0.6 mmol Ca^{2+}/kg water and 1.2 mmol Cl^-/kg water. In this simple example, sodium (Na^+) and potassium (K^+) are exchanged by calcium (Ca^{2+}) as the $CaCl^2$ enters the porous column. Initially, Na^+ present in the column. Injected Ca^{2+} is eluted as long as the exchanger contains Na^+. When the Na^+ is no longer available, K^+ is released from the exchanger. Dissolved K^+ increases above its initial concentration to balance the injected Cl^-. When all of the K^+ has been released, the concentration of Ca^{2+} increases to a steady-state value equal to the concentration of the injected solution.

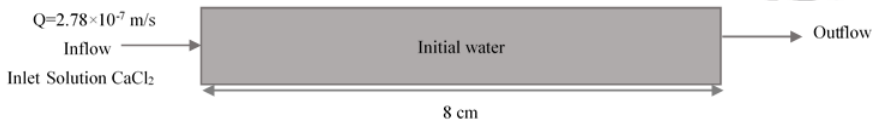

Fig. 2: Model domain and boundary conditions for transport and cation exchange problem.

We use a 2D domain with boundary conditions shown in Figure 2 within IC-FERST-REACT and compared our results against PHREEQC. Breakthrough curves for dissolved concentrations at the end of the column serve as comparison between the PHREEQC and IC-FERST-REACT. Figure 3 shows an excellent agreement between the results by PHREEQC and IC-FERST-REACT.

4.2 Calcite dissolution during CO2 geological sequestration

To show capabilities of IC-FERST-REACT in modeling mineral reaction kinetics, we considered an example involving calcite dissolution. We used a simple rectangular homogeneous medium containing mineral calcite initially saturated with water (see Figure 4). We injected a fluid with salinity of 0.05M NaCl acidified by CO_2 (pH of 5) with a pressure difference of 1 KPa. The problem is a single-phase flow and multicomponent reactive transport. Fluid properties are shown in 1.

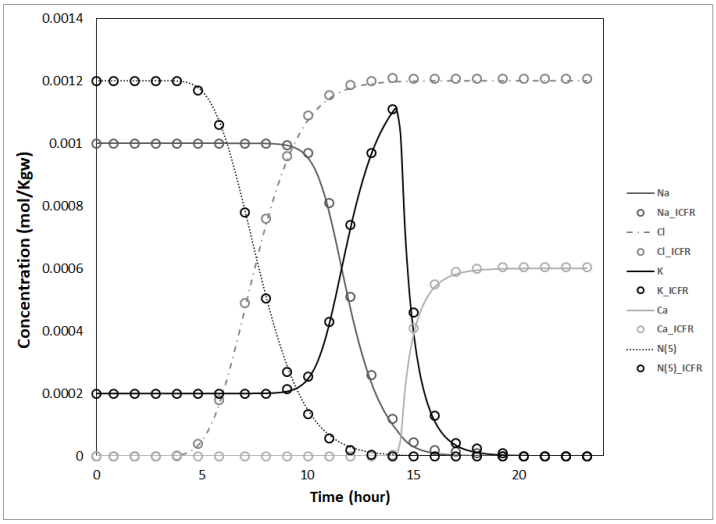

Fig. 3: Breakthrough curves at the column outlet for Cl, N (5), Na, K, and Ca. Lines show results of PHREEQC and circles show results of IC-FERST-REACT.

Calcite dissolution problem is generally presented by three reactions below [5, 34]:

$$CaCO_3 + H^+ \overset{k_1}{\rightarrow} Ca^{2+} + HCO_3^- \tag{8}$$

$$CaCO_3 + H_2CO_3 + \overset{k_2}{\rightarrow} Ca^{2+} + 2HCO_3^- \tag{9}$$

$$CaCO_3 \overset{k_3}{\rightarrow} Ca^{2+} + CO_3^{2-} \tag{10}$$

where k_1, k_2, and k_3 are the reaction rate constants. In Eq. 8, H^+ is consumed and Ca^{2+} and carbonate (HCO_3^-) are released. Calcite dissolution is kinetically described in the model using the transition state theory. The reaction rate parameters are those reported in [5]. Kinetics of calcite dissolution in CO_2-brine systems is divided into three main reaction pathways [5, 34]. In pathway 8, dissolution is independent of CO_2 pressure dominated by reaction 8. Therefore, the system is mainly pH-dependent. In pathway 9, dissolution is dependent on both pH and the CO_2 partial pressure, shown in Eq. 9. In pathway 10 calcium precipitation starts to dominate (Eq.10). The carbonate dissolution rate is represented by:

$$k = k_1\, a_{H^+} + k_2\, a_{H_2CO_3} + k_3 \tag{11}$$

where a_{H^+} and $a_{H_2CO_3}$ are the activities of hydrogen ion and carbonic acid. The kinetic coefficients reaction k_1, k_2, and k_3 are -0.05, -3.3., and -6.19 $mol/m^2 s$, respectively. Note that reaction rate depends on surface area (that was considered constant) and pH. However, it becomes almost constant at pH

above 7. Our results demonstrate the reactive transport of CO_2 and calcite and the production of Ca^{2+} and bicarbonate.

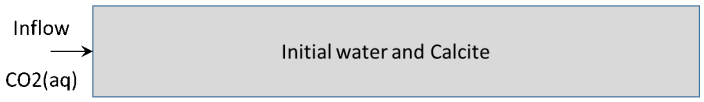

Fig. 4: Illustration of the CO_2 injection in porous medium domain that saturated with calcite and water

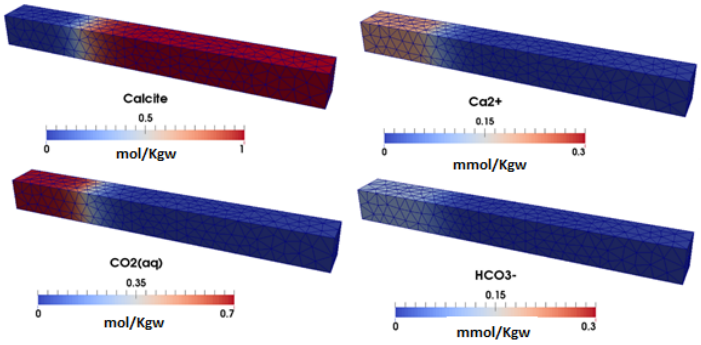

Fig. 5: Mole fraction change ($mmol/Kgw$) in calcite dissolution during CO_2 injection after 2PV injected. We compared our simulation results with the 1D transport model that solved by PHREEQC. The results are shown in Figure 6. IC-FERST-REACT results agrees well with PHREEQC.

Figure 5 illustrates the results of calcite dissolution after 2 pore volume (PV) injection of CO_2 into the medium and the release and transport of Ca^{2+} and HCO_3^- through the beam. The model that was in equilibrium before any injection and Calcite dissolution starts by injecting the CO_2 to the domain and Ca^{2+} and HCO_3^- are released in the domain (Figure 6). The graph shows the transport of the components over the domain. At the time of 2PV the pick of reaction occurred at 1PV (Figure 6). At this position the calcite and injected CO_2 are in equilibrium with water the variations of Ca^{2+} and HCO_3^- decrease until about 2PV such that there is no dissolution of calcite and therefore no release of components thereafter.

4.3 Calcite dissolution during CO_2 injection in fractured rocks

In this example, we consider a two-phase flow problem in which the non-wetting gaseous CO_2 is injected into a fractured rock (Figure 7)

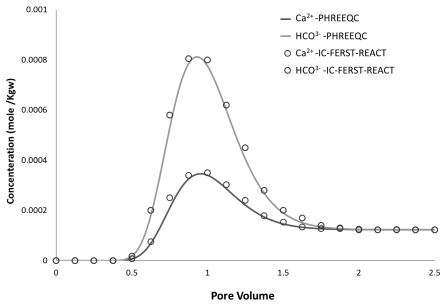

Fig. 6: Calcite dissolution during CO_2 injection at the middle of beam. Comparison between the results of IC-FERST-REACT and PHREEQC.

saturated with water. The CO_2 is injected from the left boundary while the right boundary is open to flow (Figure 7). Other boundaries are closed to flow. Fluid properties and model dimensions are shown in Table 1.

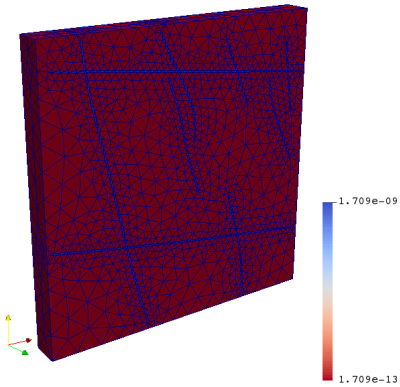

Fig. 7: Computational domain and mesh of the 3D fractured porous domain. The domain has dimensions of (0.05 x 0.5 x 0.5) and fracture aperture is 0.003 m.

Fractures are represented explicitly, but due to the use of unstructured grids the required number of elements is not necessarily high, requiring only 5649 nodes or 30912 elements (Figure 7). Initially the domain is saturated with water at pressure of 20 MPa and constant temperature of 90°C. Calcite is the only mineral phase in the domain and in fractures, **with a 100 percent concentration, and the Calcite dissolu-**

tion calculated by Kinetic control that is explained above. The CO_2 is injected with a pressure difference of 1 KPa. Figures 8 and 9 illustrate the concentration of dissolved species (i.e., CO_2 (aq), HCO_3^-, Ca^{2+}) and calcite mole fraction after dissolution in the fractured domain at about 1 PV and 1.5 PV. As expected, the results show expectedly faster displacement of gaseous CO_2 through connected fracture networks.

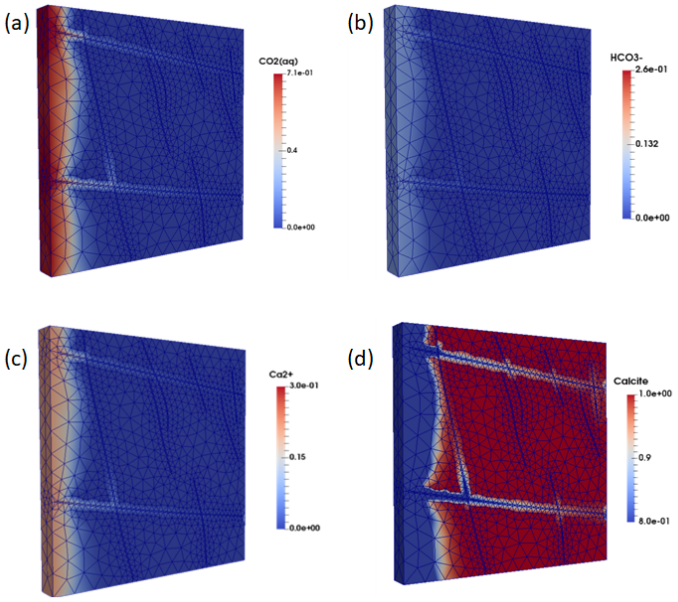

Fig. 8: Map of (a) CO_2 concentration (mol/Kgw); (b) HCO_3^- concentration ($mmol/Kgw$); (c) Ca^{2+} concentration ($mmol/Kgw$); (d) Calcite mole fraction (mol/Kgw) at 1 PVs.

We present in Figure 10 the variation of components and calcite dissolution at the end of the domain. Calcite dissolves along the fractures after having been in contact with CO_2 and release Ca^{2+} and HCO_3^- until it is in equilibrium with aqueous phase (calcite SI is zero) approximately after 2.5 PVs of injection. Simulation results illustrate that about 20 percent of calcite is dissolved in aqueous phase during CO_2 injection. **Note, that the dissolution of calcite can potentially impact the petrophysical properties and the geometry of fractures, blocking passages or enlarging others. Nonetheless that is outside of the scope of this work and will be addressed in future studies.**

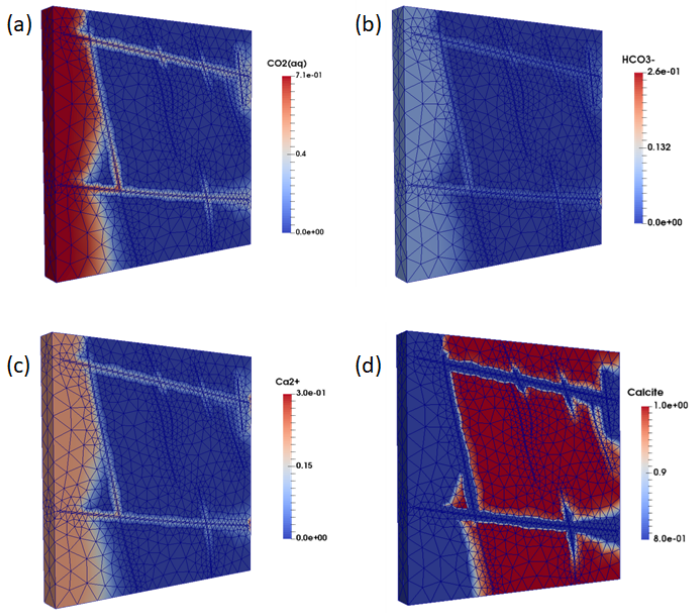

Fig. 9: Map of (a) CO_2 concentration (mol/Kgw); (b) HCO_3^- concentration $(mmol/Kgw)$; (c) Ca^{2+} concentration $(mmol/Kgw)$; (d) Calcite mole fraction (mol/Kgw) at 1.5 PVs.

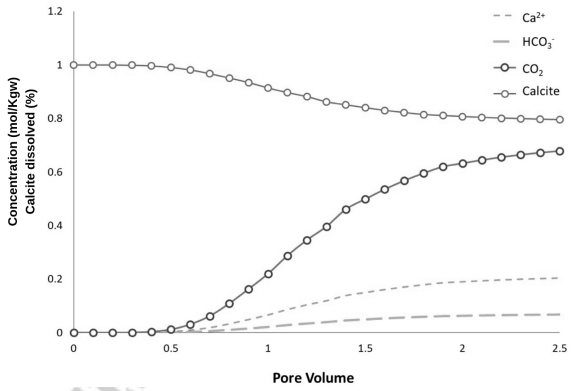

Fig. 10: Evolution of calcite dissolution in the fracture during CO_2 injection.

4.4 Faulted reservoir with contrasting permeability layers

This numerical example presents a more realistic geological domain consisting of a layered system of contrasting permeabilities that have been faulted (Figure 11). The initial mesh is generated us-

ing surface-based geological modelling following approach in [17], again the required number of elements to represent the geometry is low, see Table 1. Gaseous CO_2 is injected from the left face with the injection rate is 0.2 m^3/s. The domain is initially saturated with 0.05M $NaCl$ brine acidified by CO_2 in equilibrium with a pH of 5. Solid phase consists of calcite and the dissolution of calcite was represented by three reaction pathways in Equations 8, 9, 10.

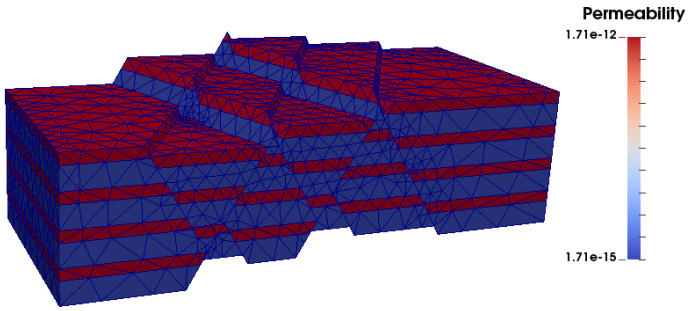

Fig. 11: Initial mesh and permeability map of 3D porous domain with fault.

As mention in subsection 2.2, DMO is one of the key features of IC-FERST and it is vital to test that IC-FERST-REACT can also use DMO. Therefore, in this example we use dynamic mesh optimization to study if IC-FERST-REACT can perform well when using DMO. The mesh is adapted to ensure that the precision of the concentration fields as well as the saturation fields are below 0.01, see [29] for more details. In comparison, using the same precision with a fixed mesh requires 125000 elements, while using DMO the average number of elements for this simulation is reduced to only 30000. This is very important when modelling reaction as the reduction of the cost is much higher due to the high cost per element to compute the equilibrium state of the components.

Figures 12 and 13 present the variations of concentration (CO_2 (aq), Ca^{2+}) in two approaches: with and without DMO respectively. Results illustrate that the displacement of CO_2 through high-permeability layer as well as dissolution of calcite and release of HCO_3^-, and Ca^{2+}. The Figures show that the results with DMO are more accurate, better representing the fronts and diminishing the mass transported thought the low permeable layers, see Figure 12 (c).

Figure 14 shows species concentration and calcite dissolution in two locations of the computational domain: one is within a high-permeability layer and one is within a low-permeability layer.

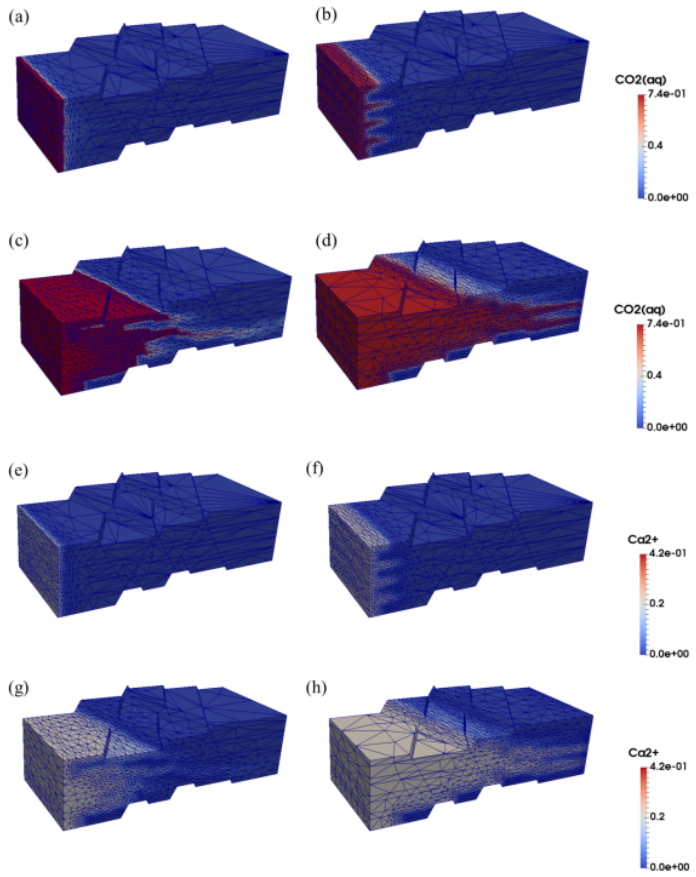

Fig. 12: (a-d) Dissolved CO_2 concentration (mol/Kgw), and (e-h) Ca^{2+} concentration ($mmol/Kgw$) with mesh adaptivity at 1, 2, 4, and 6 PV injection.

Figure 15 presents the difference between using DMO on the results of CO_2 concentration. **The results show that the difference is negligible. Thus, modeling with DMO is valid and it helps to reduce both the cost of modeling and also the costs associated with reaction computations.**

5 Discussion

The use of unstructured meshes and DMO for modelling multiphase porous media flow has already been shown to be useful to better represent geological features with a reduced number of elements, as unstructured grids are not constrained by the two-point flux approximation scheme [16]. In this approach, the mesh has to capture the the geology being represented and not the opposite. This approach

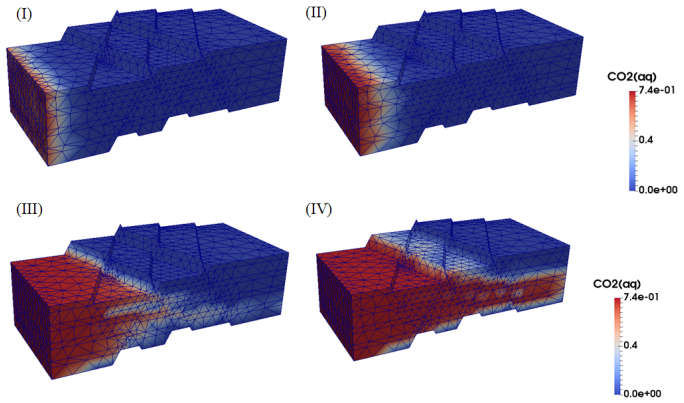

Fig. 13: (I-IV) Dissolved CO_2 concentration (mol/Kgw) without mesh adaptivity

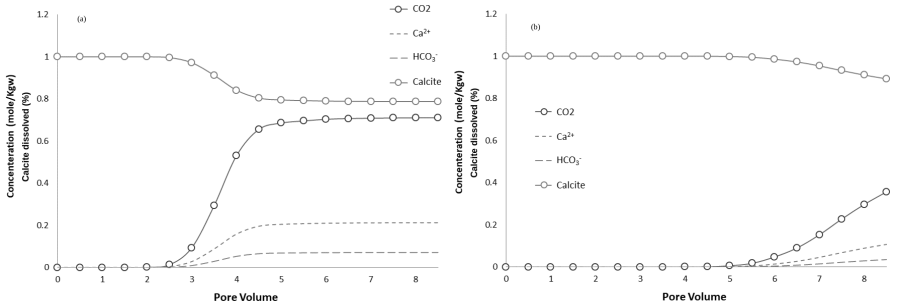

Fig. 14: Dissolved species concetration during CO_2 injection: A CV is within a (a) high-permeability, (b) low-permeability layer.

requires geological features to be represented in a mesh-less fashion, in our case we use surface-based modelling [17] represented using NURBS. The use of DMO does not alter the geology as the surfaces are not modified by the mesh adaptivity routine. Moreover, it helps to reduce the number of elements required even further by only placing the resolution when and where it is necessary. Considering how expensive reaction calculation can be (from 75 to 99 percent of the total simulation [41, 52]), the use of DMO for reactive flows has the potential to severely decrease the computational cost associated with reactive flows. In view of the fact that reactions occur at the CV level, coupling a readily available package such as PHREEQCRM (with its database of reactions included) is straightforward, even though IC-FERST uses unstructured adaptive meshes. In this way, the coupling is the same as it would be with a structured-based

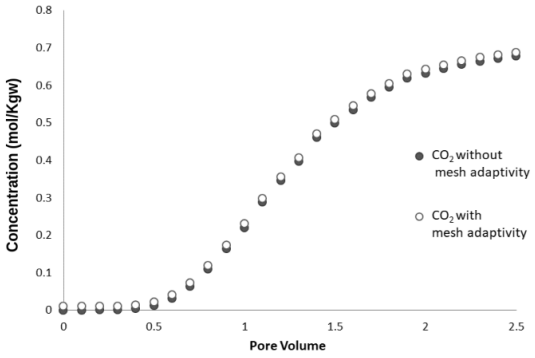

Fig. 15: CO_2 injection at the grid cell within high-permeability layer in two different model: with and without mesh adaptivity.

code. Parallelisation of the procedure is also trivial as again, only IC-FERST requires information of neighbouring elements/CVs and we expect to have the same performance with IC-FERST-REACT than that obtained by IC-FERST in parallel [38]. The presented work here is the first step to show that reaction with DMO and surface based modelling is not only feasible but also very efficient. The main challenges ahead to ensure that this approach is feasible are: (i) to consider variations of the petrophysical properties of the domain and (ii) to implement a two way coupling version (SIA). Regarding (i) this is a hard challenge as one of the axioms of surface-based modelling is to consider constant properties within a domain region, which is also used by DMO to ensure that no petrophysical properties need to be interpolated between meshes [16]. However challenging this is, some possibilities are already available such as fixing the mesh in those areas where petrophysical properties occur. This will limit the flexibility of DMO partially, but will ensure that the results are correct and is efficient to implement. Other possibility is to update the surfaces after few time-levels, or a combination of both. Regarding (ii), we do not expect to encounter challenges different to those already found by others coupling fluid codes to reactive packages.

Despite the known extra costs associated with the use of unstructured mesh when compared with fix meshes, the fact that in reactive flows reaction calculations can take the majority of the computational costs means that DMO is potentially more useful than for non-reactive flows as ir reduces the overall elements, and therefore, the required reactive computations. The results presented here in model 4.4 show that the model using DMO requires 4 times fewer elements that the one using a fixed mesh with equivalent precision.

6 Conclusions

In this study we have presented and tested an approach through which the USGS geochemical reaction package, PHREEQCRM, is coupled to IC-FERST for reactive transport modeling. The proposed coupling procedure can be used to model different reactive transport problems as a one-way coupling approach. We are in developing stage for our iterative coupling between these two codes as well as developing a fully coupled framework. We first validated IC-FERST-REACT by comparing its performance against PHREEQC for ion exchange as well as calcite dissolution problem. One of our specific goals in this work was to model mineral dissolution occurring during CO_2 geological sequestration within heterogeneous media. We focused on heterogeneous media with fractures and faults to better understand the variation of minerals and within fractures which provide fast flow pathways for gaseous CO_2.This work presents our initial effort. Our study is the first work to our knowledge that present coupling a multiphase flow code with dynamic mesh optimization capabilities to a reaction package. Considering the high computational cost of calculating the reaction processes, the use of dynamic mesh optimization represents an excellent opportunity to lessen this cost by reducing the number of elements required to model a very complex geological medium.

Acknowledgements The Funding from EPSRC (Smart-GeoWells grant EP/R005761/1) is gratefully acknowledged. We would also like to thank H. Osman for providing the geometry and mesh for the fractured rock test case.

References

1. Bahlali, M.L., Hamzehloo, A., Salinas, P., Butler, A.P., Jackson, M.D., Jacquemyn, C., Pain, C.C.: Dynamic mesh optimization and parallel computing for groundwater flow modelling: Saline intrusion. Under review (2020)
2. Brooks, R., Corey, A.: Hydrology Papers, vol. 3, chap. Hydraulic properties of porous media. Colorado State University (1964)
3. Carrayrou, J., Hoffmann, J., Knabner, P., Kräutle, S., De Dieuleveult, C., Erhel, J., Van Der Lee, J., Lagneau, V., Mayer, K.U., Macquarrie, K.T.B.: Comparison of numerical methods for simulating strongly non-linear and heterogeneous reactive transport problems – the MoMaS benchmark case. Computational Geosciences **14**, 483–502 (2010). DOI 10.1007/s10596-010-9178-2. URL https://hal-mines-paristech.archives-ouvertes.fr/hal-00505371
4. Charlton, S.R., Parkhurst, D.L.: Modules based on the geochemical model phreeqc for use in scripting and programming languages. Computers & Geosciences **37**(10), 1653–1663 (2011)
5. Chou, L., Garrels, R.M., Wollast, R.: Comparative study of the kinetics and mechanisms of dissolution of carbonate minerals. Chemical Geology **78**(3), 269 – 282 (1989). DOI https://doi.org/10.1016/0009-2541(89)90063-6. Kinetic Geochemistry
6. Dai, Z., Samper, J.: Inverse problem of multicomponent reactive chemical transport in porous media: Formulation and applications. Water Resources Research **40**(7) (2004). DOI 10.1029/2004WR003248
7. DePaolo, D.J., Cole, D.R.: Geochemistry of geologic carbon sequestration: an overview. Reviews in Mineralogy and Geochemistry **77**(1), 1–14 (2013)

8. Durlofsky, L.: A triangle based mixed finite element finite volume technique for modelling two-phase flow through porous media. Journal Computational Physics **105**, 252–266 (1993)
9. Farrell, P., Maddison, J.: Conservative interpolation between volume meshes by local galerkin projection. Computer Methods in Applied Mechanics and Engineering **200**(1-4), 89 – 100 (2011). DOI http://dx.doi.org/10.1016/j.cma.2010.07.015
10. Forsyth, P.A.: A Control Volume Finite Element Approach to NAPL Groundwater Contamination (1991). DOI 10.1137/0912055
11. Geiger, S., Roberts, S., Matthai, S., Zoppou, C., A. Burri, A.: Combining finite element and finite volume methods for efficient multiphase flow simulations in highly heterogeneous and structurally complex geologic media. Geofluids **4**(4), 284–299 (2004)
12. Gomes, J., Pavlidis, D., Salinas, P., Xie, Z., Percival, J., Melnikova, Y., Pain, C., Jackson, M.D.: A force-balanced control volume finite element method for multiphase porous media flow modelling. Int. J. Numer. Meth. Fluids **83**, 431–445 (2017). DOI 10.1002/fld.4275
13. Hammond, G.E., Lichtner, P.C., Mills, R.: Evaluating the performance of parallel subsurface simulators: An illustrative example with pflotran. Water resources research **50**(1), 208–228 (2014)
14. Hao, Y., Sun, Y., Nitao, J.J.: Overview of NUFT: A Versatile Numerical Model for Simulating Flow and Reactive Transport in Porous Media (2012). DOI 10.2174/978160805306311201010212
15. Hosseini, S.A., Lashgari, H., Choi, J.W., Nicot, J.P., Lu, J., Hovorka, S.D.: Static and dynamic reservoir modeling for geological co2 sequestration at cranfield, mississippi, usa. International Journal of Greenhouse Gas Control **18**, 449–462 (2013)
16. Jackson, M.D., Percival, J., Mostaghimi, P., Tollit, B., D. Pavlidis, C.P., Gomes, J., El-Sheikh, A., P. Salinas, A.M., Blunt, M.: Reservoir modeling for flow simulation by use of surfaces, adaptive unstructured meshes, and an overlapping-control-volume finite-element method. SPE Reservoir Evaluation and Engineering **18** (2015). DOI 10.2118/163633-PA
17. Jacquemyn, C., Hampson, G.J., Jackson, M.D.: Surface-based geological reservoir modelling using grid-free nurbs curves and surfaces. Mathematical Geosciences (2019). DOI 10.1007/s11004-018-9764-8
18. Kampitsis, A.E., Adam, A., Salinas, P., Pain, C.C., Muggeridge, A.H., Jackson, M.D.: Dynamic adaptive mesh optimisation for immiscible viscous fingering. Computational Geosciences **24**(3), 1221–1237 (2020). DOI 10.1007/s10596-020-09938-5. URL https://doi.org/10.1007/s10596-020-09938-5
19. Kolditz, O., Bauer, S., Bilke, L., Böttcher, N., Delfs, J.O., Fischer, T., Görke, U.J., Kalbacher, T., Kosakowski, G., McDermott, C.I., Park, C.H., Radu, F., Rink, K., Shao, H., Shao, H.B., Sun, F., Sun, Y.Y., Singh, A.K., Taron, J., Walther, M., Wang, W., Watanabe, N., Wu, Y., Xie, M., Xu, W., Zehner, B.: Opengeosys: an open-source initiative for numerical simulation of thermo-hydro-mechanical/chemical (thm/c) processes in porous media. Environmental Earth Sciences **67**(2), 589–599 (2012). DOI 10.1007/s12665-012-1546-x
20. Kolditz, O., Bauer, S., Bilke, L., Grunwald, N., Delfs, J.O., Fischer, T., Görke, U., Kalbacher, T., Kosakowski, G., Mcdermott, C., Park, C.H., Radu, F., Rink, K., Shao, H., Sun, F., Sun, Y., Singh, A., Taron, J., Walther, M., Zehner, B.: Opengeosys: An open-source initiative for numerical simulation of thermo-hydro-mechanical/chemical (thm/c) processes in porous media. Environmental Earth Sciences **67**, 589–599 (2012). DOI 10.1007/s12665-012-1546-x
21. Korrani, A.K.N., Sepehrnoori, K., Delshad, M.: Coupling iphreeqc with utchem to model reactive flow and transport. Computers & Geosciences **82**, 152–169 (2015)
22. Lichtner, P.C.: The Quasi-Stationary State Approximation to Fluid/Rock Reaction: Local Equilibrium Revisited, pp. 452–560. Springer US, New York, NY (1991). DOI 10.1007/978-1-4613-9019-0_13. URL https://doi.org/10.1007/978-1-4613-9019-0_13
23. Millington, R.J., Quir, J.P.: Permeability of porous solids. Transactions of the Faraday Society (1961)
24. Mohammadi, H., Delshad, M., Pope, G.A., et al.: Mechanistic modeling of alkaline/surfactant/polymer floods. SPE Reservoir Evaluation & Engineering **12**(04), 518–527 (2009)

25. Navarre-Sitchler, A., Steefel, C.I., Sak, P.B., Brantley, S.L.: A reactive-transport model for weathering rind formation on basalt. Geochimica et Cosmochimica Acta **75**(23), 7644 – 7667 (2011). DOI https://doi.org/10.1016/j.gca.2011.09.033. URL http://www.sciencedirect.com/science/article/pii/S0016703711005540
26. Noiriel, C., Steefel, C.I., Yang, L., Ajo-Franklin, J.: Upscaling calcium carbonate precipitation rates from pore to continuum scale. Chemical Geology **318-319**, 60 – 74 (2012). DOI https://doi.org/10.1016/j.chemgeo.2012.05.014
27. Obeysekara, A., Lei, Q., Salinas, P., Pavlidis, D., Xiang, J., Latham, J.P., Pain, C.: Modelling stress-dependent single and multi-phase flows in fractured porous media based on an immersed-body method with mesh adaptivity. Computers and Geotechnics **103**, 229 – 241 (2018). DOI https://doi.org/10.1016/j.compgeo.2018.07.009. URL http://www.sciencedirect.com/science/article/pii/S0266352X18301824
28. Ortoleva, P., Merino, E., Moore, C., Chadam, J.: Geochemical self-orginisation I: Reaction-transport feedbacks and modelling approach. American Journal of Science **287**, 979–1007 (1987)
29. Pain, C., Umpleby, A., de Oliveira, C., Goddard, A.: Tetrahedral mesh optimisation and adaptivity for steady-state and transient finite element calculations. Computer Methods in Applied Mechanics and Engineering **190**, 3771–3796 (2001). DOI 10.1016/S0045-7825(00)00294-2
30. Parkhurst, D., Appelo, C.: Description of input and examples for PHREEQC version 3—A computer program for speciation, batch-reaction, one-dimensional transport, and inverse geochemical calculations (2013). URL https://pubs.usgs.gov/tm/06/a43/
31. Parkhurst, D.L., Appelo, C.: Description of input and examples for phreeqc version 3: a computer program for speciation, batch-reaction, one-dimensional transport, and inverse geochemical calculations. Tech. rep., US Geological Survey (2013)
32. Parkhurst, D.L., Appelo, C., et al.: User's guide to phreeqc (version 2): A computer program for speciation, batch-reaction, one-dimensional transport, and inverse geochemical calculations. Water-resources investigations report **99**(4259), 312 (1999)
33. Parkhurst, D.L., Wissmeier, L.: Phreeqcrm: A reaction module for transport simulators based on the geochemical model phreeqc. Advances in Water Resources **83**, 176–189 (2015)
34. Plummer, L.N., Wigley, T.M.L., Parkhurst, D.L.: The kinetics of calcite dissolution in CO 2 -water systems at 5 degrees to 60 degrees C and 0.0 to 1.0 atm CO 2. American Journal of Science **278**(2), 179–216 (1978). DOI 10.2475/ajs.278.2.179
35. Prommer, H., Barry, D., Davis, G.: A one-dimensional reactive multi-component transport model for biodegradation of petroleum hydrocarbons in groundwater. Environmental Modelling & Software **14**(2-3), 213–223 (1998)
36. Pyrcz, M.J.: A Short Note on the Generation of Geologically Realistic Stochastic Models. Center for Computational Geostatistics Annual Report Papers (August), 1–3 (2002). URL papers2://publication/uuid/59D80B79-0D65-4B52-AC2D-188D9F6AABFA
37. Salinas, P., Jacquemyn, C., Heaney, C., Pavlidis, D., Pain, C., Jackson, M.: Simulation of enhanced geothermal systems using dynamic unstructured mesh optimisation **2018**(1), 1–5 (2018). DOI https://doi.org/10.3997/2214-4609.201800949. URL https://www.earthdoc.org/content/papers/10.3997/2214-4609.201800949
38. Salinas, P., Jacquemyn, C., Kampitsis, A., Via-Estrem, L., Heaney, C., Pain, C.C., Jackson, M.D.: A Parallel Load-Balancing Reservoir Simulator with Dynamic Mesh Optimisation. In: SPE Reservoir Characterisation and Simulation Conference and Exhibition. Society of Petroleum Engineers (2019). DOI doi.org/10.2118/196664-MS
39. Salinas, P., Pavlidis, D., Xie, Z., Jacquemyn, C., Melnikova, Y., Pain, C.C., Jackson, M.D.: Improving the robustness of the control volume finite element method with application to multiphase porous media flow. International Journal for Numerical Methods in Fluids **85**, 235–246 (2017). DOI 10.1002/fld.4381
40. Seigneur, N., Mayer, K.U., Steefel, C.I.: Reactive transport in evolving porous media. Reviews in Mineralogy and Geochemistry **85**(1), 197–238 (2019)
41. Shi, Y., Liang, L., Ge, H.W., Reitz, R.D.: Acceleration of the chemistry solver for modeling di engine combustion using dynamic adaptive chemistry (dac) schemes. Combustion Theory and Modelling **14**(1), 69–89 (2010). DOI 10.1080/13647830903548834

42. Soltanian, M.R., Hajirezaie, S., Hosseini, S.A., Dashtian, H., Amooie, M.A., Meyal, A., Ershadnia, R., Ampomah, W., Islam, A., Zhang, X.: Multicomponent reactive transport of carbon dioxide in fluvial heterogeneous aquifers. Journal of Natural Gas Science and Engineering **65**, 212 – 223 (2019). DOI https://doi.org/10.1016/j.jngse.2019.03.011
43. Soltanian, M.R., Ritzi, R.W., Huang, C.C., Dai, Z.: Relating reactive solute transport to hierarchical and multiscale sedimentary architecture in a l agrangian-based transport model: 2. particle displacement variance. Water Resources Research **51**(3), 1601–1618 (2015)
44. Steefel, C., Appelo, C., Arora, B., Jacques, D., Kalbacher, T., Kolditz, O., Lagneau, V., Lichtner, P., Mayer, K.U., Meeussen, J., et al.: Reactive transport codes for subsurface environmental simulation. Computational Geosciences **19**(3), 445–478 (2015)
45. Steefel, C., Lichtner, P.: Multicomponent reactive transport in discrete fractures: Ii: Infiltration of hyperalkaline groundwater at maqarin, jordan, a natural analogue site. Journal of Hydrology **209**(1), 200 – 224 (1998). DOI https://doi.org/10.1016/S0022-1694(98)00173-5
46. Steefel, C.I.: CrunchFlow Software for Modeling Multicomponent Reactive Flow and Transport (2009). URL https://www.netl.doe.gov/sites/default/files/netl-file/CrunchFlow-Manual.pdf
47. Steefel, C.I., Druhan, J.L., Maher, K.: Modeling coupled chemical and isotopic equilibration rates. Proc Earth Planet Sci **10**, 208–217 (2014)
48. Steefel, C.I., Lasaga, A.C.: Putting transport into water-rock interaction models. Geology **20**(8), 680 (1992). DOI 10.1130/0091-7613(1992)020⟨0680:PTIWRI⟩2.3.CO;2
49. Steefel, C.I., Lasaga, A.C.: A coupled model for transport of multiple chemical species and kinetic precipitation/dissolution reactions with application to reactive flow in single phase hydrothermal systems. American Journal of Science **294**(5), 529–592 (1994). DOI 10.2475/ajs.294.5.529. URL http://www.ajsonline.org/content/294/5/529.short
50. Steefel, C.I., Lichtner, P.C.: Diffusion and reaction in rock matrix bordering a hyperalkaline fluid-filled fracture. Geochimica et Cosmochimica Acta **58**(17), 3595 – 3612 (1994). DOI https://doi.org/10.1016/0016-7037(94)90152-X
51. Steefel, C.I., MacQuarrie, K.T.: Approaches to modelling reactive transport in porous media. Reviews in Mineralogy **34**, 83–129 (1996)
52. Tonse, S.R., Moriarty, N.W., Frenklach, M., Brown, N.J.: Computational economy improvements in prism. International Journal of Chemical Kinetics **35**(9), 438–452 (2003). DOI 10.1002/kin.10140
53. Van Der Lee, J., De Windt, L., Lagneau, V., Goblet, P.: Presentation and application of the reactive transport code hytec. In: Developments in Water Science, vol. 47, pp. 599–606. Elsevier (2002)
54. White, M.D., Fang, Y.: STOMP-ECKEChem: An Engineering Perspective on Reactive Transport in Geologic Media (2012). DOI 10.2174/978160805306311201010112
55. White, M.D., McGrail, B.P.: Stomp subsurface transport over multiple phases version 1.0 addendum: Eckechem equilibrium-conservation-kinetic equation chemistry and reactive transport (2005). DOI 10.2172/976999
56. White, M.D., Oostrom, M.: Stomp subsurface transport over multiple phases version 3.0 user's guide. Tech. rep., Pacific Northwest National Lab., Richland, WA (US) (2003)
57. Yabusaki, S.B., Wilkins, M.J., Fang, Y., Williams, K.H., Arora, B., Bargar, J., Beller, H.R., Bouskill, N.J., Brodie, E.L., Christensen, J.N., et al.: Water table dynamics and biogeochemical cycling in a shallow, variably-saturated floodplain. Environmental science & technology **51**(6), 3307–3317 (2017)
58. Yapparova, A., Gabellone, T., Whitaker, F., Kulik, D.A., Matthäi, S.K.: Reactive transport modelling of dolomitisation using the new csmp++ gem coupled code: Governing equations, solution method and benchmarking results. Transport in Porous Media **117**(3), 385–413 (2017)
59. Yapparova, A., Gabellone, T., Whitaker, F., Kulik, D.A., Matthäi, S.K.: Reactive transport modelling of hydrothermal dolomitisation using the csmp++gem coupled code: Effects of temperature and geological heterogeneity. Chemical Geology **466**, 562 – 574 (2017). DOI https://doi.org/10.1016/j.chemgeo.2017.07.005
60. Zhang, G., Lu, D., Ye, M., Gunzburger, M., Webster, C.: An adaptive sparse-grid high-order stochastic collocation method for bayesian inference in groundwater reactive transport modeling. Water Resources Research **49**(10), 6871–6892. DOI 10.1002/wrcr.20467

61. Zyvoloski, G.: Fehm: A control volume finite element code for simulating subsurface multi-phase multi-fluid heat and mass transfer (2007)